

Precision measurement of the Z boson to electron neutrino coupling at the future circular colliders^{*}

R. Aleksan^a and S. Jadach^b

^a*IRFU, CEA, Université Paris-Saclay, 91191 Gif-sur-Yvette cedex, France*

^b*Institute of Nuclear Physics, Polish Academy of Sciences,
ul. Radzikowskiego 152, 31-342 Kraków, Poland*

Abstract

At the high luminosity electron-positron circular colliders like FCC-ee in CERN and CEPC in China it will be possible to measure very precisely $e^+e^- \rightarrow Z\gamma$ process with subsequent Z decay into particles invisible in the detector, that is into three neutrinos of the Standard Model and possibly into other weakly coupled neutral particles. Apart from the measurement of the total invisible width (which is not the main subject of this work) this process may be used as a source of Z coupling to electron neutrino – known very poorly. This is possible due to the presence of the t -channel W exchange in the $e^+e^- \rightarrow \nu_e\bar{\nu}_e\gamma$ channel which deforms slightly spectrum of the photon. We are going to show experimental investigation of this effect, for ~ 10 inverse atobarn accumulated luminosity, which can provide measurement of the $Z - \nu_e$ coupling with statistical error of order 1%. The estimation of the systematic experimental error will require more work, but most likely it will be of similar size.

^{*}This work is partly supported by the Polish National Science Center grant 2016/23/B/ST2/03927 and the CERN FCC Design Study Programme.

1 Introduction

Recent measurements in the B meson sector have shown evidences for lepton universality violation at the 3 to 4 standard deviations (σ) levels. Without being exhaustive, deviations from the Standard Model (SM) are observed by comparing semileptonic B decays $B \rightarrow D^{(*)}\tau\nu$ on the one hand, and $B \rightarrow D^{(*)}\ell\nu$ with $\ell = \mu, e$ on the other hand [1–5]. Discrepancies are also observed in comparing the decays $B \rightarrow K^{(*)}\mu\nu$ and $B \rightarrow K^{(*)}e\nu$ [6–8]. In contrast, lepton universality is verified at the 1% and 0.1% level in W and Z decays respectively, involving charged leptons [9], although there is a slight tension at the 3σ level in the W decay $W \rightarrow \tau\nu$ versus the average $W \rightarrow \ell\nu$ ($\ell = \mu, e$). In the same vein, one notes that neutrino counting in Z decays shows a very slight deficit (2σ), with $N_\nu = 2.984 \pm 0.008$ [9]. (Although, corrections due to beam-beam effects of recent Ref. [10] change this result to $N_\nu = 2.992 \pm 0.008$.) Therefore, to shed further light in this area and complement these tests, the precision of which should be considerably improved in the near and long term future at HL-LHC, SuperKEKB and FCC, it might be very useful to study universality in $Z \rightarrow \nu_\ell \bar{\nu}_\ell$ decays. In general, this is a non trivial task since neutrinos are difficult to detect and thus is the identification of their species. In this paper we investigate a method to achieve this objective by “making the neutrino flavors visible in Z decays”. The future high-energy circular electron-positron collider FCC-ee [11–13] would be an ideal tool for this purpose.

2 Testing Universality of neutrinos in Z^0 decays

The charged and neutral current interaction of neutrino have been observed since a long time in fixed target experiments using muon neutrino beams. Although the production of a charged lepton in the final state tags the incoming neutrino flavor in charged current interaction for Deep Inelastic Scattering (DIS) events, the same procedure cannot be used in neutral current since the final state neutrino is not detected. The flavor is only inferred indirectly by comparing the neutral current events to the SM expectations. More recently, the SNO experiment has measured the charged and neutral current interactions of solar electron neutrinos. The comparison of the respective rates has shown that different types of neutrinos are involved in neutral current events [14] than the one (ν_e) observed in charged current. But here again, the flavor of the neutrinos interacting in the neutral current events is not identified and thus any extraction of $Z\nu\nu$ coupling is theory dependent. Furthermore the uncertainty on the incoming neutrino flux does not enable very precise measurements. The overall situation is summarized by the Particle Data Group [9] for the Z couplings to ν_e and ν_μ as follows:

$$\begin{aligned} g_Z^{\nu_e} &= 1.06 \pm 0.18 \\ g_Z^{\nu_\mu} &= 1.004 \pm 0.034 \end{aligned} \tag{2.1}$$

In the following we are going to present a method to measure the individual $Z\nu_e\nu_e$ coupling, which is so far poorly measured.

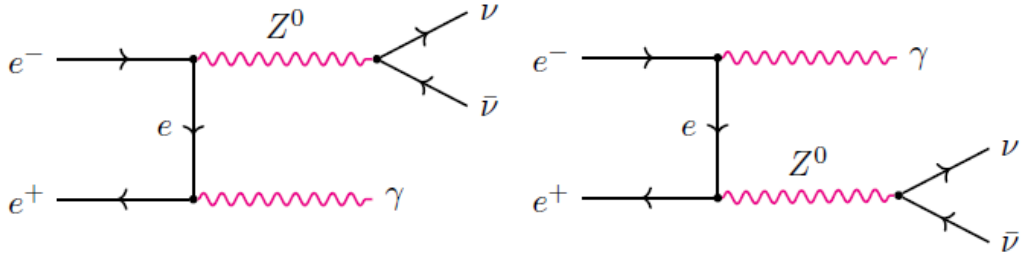


Figure 1: Production of flavor-untagged ν through the process $e^+e^- \rightarrow Z^0\gamma \rightarrow \nu\bar{\nu}\gamma$.

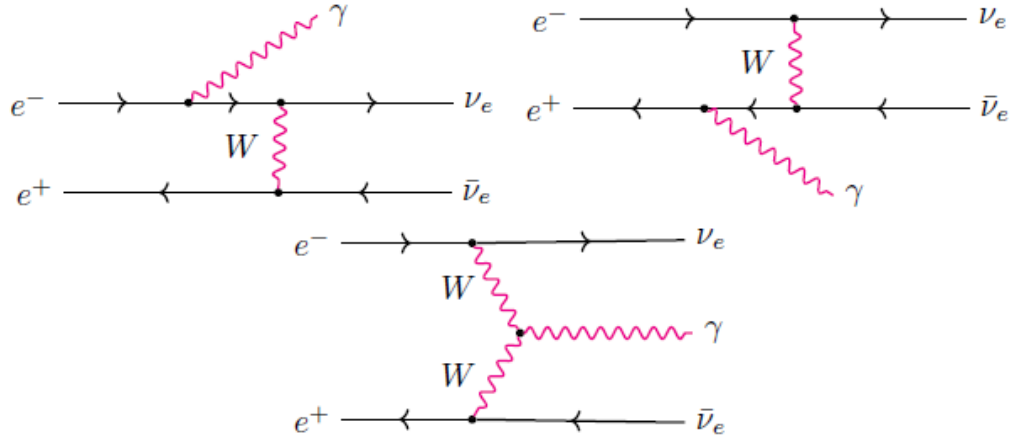


Figure 2: Production of flavor-tagged ν_e through the process $e^+e^- \rightarrow \nu_e\bar{\nu}_e\gamma$ with W exchange.

3 The method

The combined strength of couplings of Z boson to all particles contributing to Z invisible width was at LEP experiments conveniently parametrized [15] in terms the so called neutrino number parameter N_ν , equal 3 in the SM.

Two sensitive ways to measure N_ν have been used in the past:

1. Precise determination of the Z^0 production peak in e^+e^- collisions and the Z line shape. This is the most precise method with $N_\nu = 2.984 \pm 0.008$ [9, 15], thanks to the statistics and the precise beam energy determination at LEP.
2. Identification and counting of the Z boson radiative return (ZRR) process in a center of mass energy above the Z -pole, i.e. using Initial State Radiation (ISR) $e^+e^- \rightarrow \gamma X$, see diagrams in Figure 1. LEP has measured $N_\nu = 2.92 \pm 0.05$ [9, 16].

However in both cases, one has only derived the total number of light neutrino species (N_ν) assuming universality of the Z coupling to the neutrino species, i.e. without measuring the individual couplings. Indeed, by determining the Z production peak cross section and the Z width, one deduces its invisible cross section.

$$\begin{aligned} \sigma(e^+e^- \rightarrow Z \rightarrow \text{invisible}) = \\ (g_Z^{\nu_e} \mathcal{A}_Z^{\nu_e})^2 + (g_Z^{\nu_\mu} \mathcal{A}_Z^{\nu_\mu})^2 + (g_Z^{\nu_\tau} \mathcal{A}_Z^{\nu_\tau})^2 + (g_Z^X \mathcal{A}_Z^X)^2, \end{aligned} \quad (3.1)$$

where g_Z^ν and \mathcal{A}_Z^ν are the individual couplings of Z to neutrinos and the well know Breit-Wigner amplitudes respectively. Similarly g_Z^X and \mathcal{A}_Z^X are related to Z decays to invisible new physics, which couples to Z , if any. Since all \mathcal{A}_Z are identical for fermions, one gets

$$N_\nu \sim (g_Z^{\nu_e})^2 + (g_Z^{\nu_\mu})^2 + (g_Z^{\nu_\tau})^2 + (g_Z^X)^2 \quad (3.2)$$

Normalizing SM couplings to one, $g_Z^{\nu_e} = g_Z^{\nu_\mu} = g_Z^{\nu_\tau} = 1$ and $g_Z^X = 0$, one obtains $N_\nu = 3$.

At FCC-ee [11–13], a very significant improvement (by several orders of magnitude) is expected for the determination of N_ν , due to high luminosities achievable around the Z -pole and at higher energy and reduction of the experimental and theory uncertainties [17].

Obviously, there is no means of discriminating one coupling constant from another in the process of Figure 1, since only the sum of the couplings is measured. For the following in this paper, let us define the parameter η rescaling Z couplings as follows

$$g_Z^{\nu_e} = \sqrt{1+\eta}, \quad g_Z^{\nu_\mu} = 1, \quad g_Z^{\nu_\tau} = \sqrt{1-\eta}, \quad (3.3)$$

where the deviation of $g_Z^{\nu_e}$ from the SM is compensated by the opposite deviation of $g_Z^{\nu_\tau}$, while keeping constant more precisely measured total invisible Z width and $g_Z^{\nu_\mu}$.

The important point is that in the $e^+e^- \rightarrow \nu_e \bar{\nu}_e \gamma$ process there are additional diagrams producing electron neutrinos in the final state, with t -channel W_t boson exchange, see Figure 2. These diagrams interfere with the ones in Figure 1. Therefore, observing this interference in the γ energy spectrum related to the $\nu\bar{\nu}$ invariant mass¹,

$$M_{\nu\bar{\nu}}^2 \simeq s - 2\sqrt{s}E_\gamma \quad \text{or} \quad v = \frac{E_\gamma}{E_{beam}} \simeq 1 - \frac{M_{\nu\bar{\nu}}^2}{s}, \quad (3.4)$$

would lead to the measurement of the $Z - \nu_e$ coupling ($g_Z^{\nu_e}$), as aimed in this paper. We shall refer in the following to this interference in short as $Z_s \otimes W_t$ interference.

In the left part of Fig 3 we show how big is the effect of the t -channel W -exchange contribution of Figure 2 comparing Born cross section $\sigma^{Born}(M_{\nu\bar{\nu}}^2)$ for $\nu = \nu_e$ and $\nu = \nu_\mu$ near the Z peak, that is in the range $|v - v_Z| \leq 0.02$, $v_Z = 1 - M_Z^2/s$, which translates into $88.299 \geq M_{\nu\bar{\nu}} \geq 93.987$ for $s^{1/2} = 161\text{GeV}$. The relative effect of the W -exchange with respect to all 3 neutrino case is up to 8%, changing sign in the middle of the Z peak. Born cross section is calculated using expressions of eqs. (2.9-2.11) in Ref. [18]. We

¹Here and in the following E_γ is total energy of one or more photons detected above certain minimum energy and minimum angle from the beams in the ZRR process. Should there be multiple γ , an additional term proportional to $M_{n\gamma}^2$ is present but can be safely neglected as it is very small.

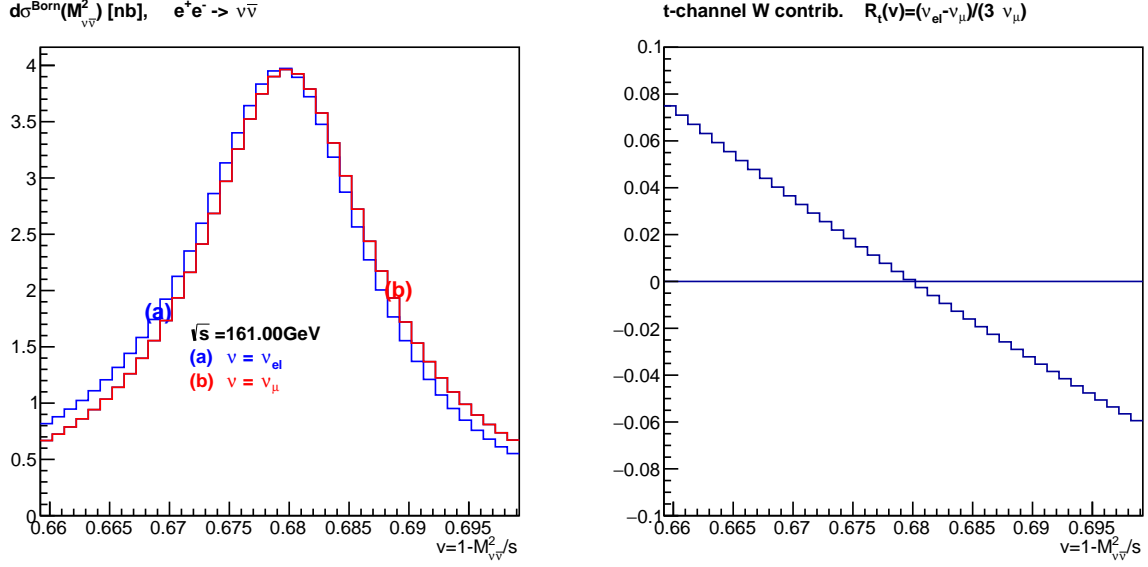


Figure 3: The LHS plot shows $\sigma^{Born}(M_{\nu\bar{\nu}}^2)$ for $e^+e^- \rightarrow \nu\bar{\nu}$, $\nu = \nu_e, \nu_\mu$ as function of variable $v = 1 - M_{\nu\bar{\nu}}^2/s$, for $s^{1/2} = 161\text{GeV}$, the same as in the following MC results for ZRR process. The RHS plot illustrates relative contribution of the t -channel W -exchange diagram in the Born cross section for all three neutrinos.

have checked that we reproduce benchmark Table 1 of Born cross sections and forward-backward asymmetries² in this paper.

From Figure 3 it is obvious that in the ZRR process our aim will be to measure asymmetric deformation of the Z resonance shape in the photon spectrum, that is its *skewness*. Of course, QED effects will also contribute to the skewness of the Z lineshape ZRR spectrum, hence very good quality MC program for the ZRR of the KKMC class [19], or even better, will be indispensable to sort out QED effects in the FCC-ee data analysis.

The contribution of the W -exchange diagram near the Z -peak is almost entirely due to the interference of the dominant s -channel Z -resonant amplitude (which contains precious coupling of the Z to electron neutrino) and the trivial W -exchange diagram, as seen clearly from the presence of the zero in the middle of the Z peak – while W -exchange diagram squared is negligible.

The diagram contribution pattern is quite different for ZRR at low v and high $M_{\nu\bar{\nu}}$, where W -exchange diagram dominates over the Z -resonant diagram by order of magnitude³. Again, it is the interference of the two, which could provide valuable information on the Z couplings to electron neutrino. Due to much smaller cross sections this option looks less attractive, nevertheless it requires quantitative study in the future.

The issue of how the invisible width of Z boson parametrized in terms of N_ν could indicate New Physics was elaborated in many papers, see for instance Refs. [20, 21]. The

²In Ref. [18] it was obtained in using non-MC programs **KKsem** and **ZFITTER**.

³For example in the range $v \in (0.2, 0.4)$ corresponding to $M_{\nu\bar{\nu}} \in (125, 144)\text{GeV}$ at $s^{1/2} = 161\text{GeV}$.

present work is the first dedicated study on how to extract Z coupling to electron neutrino taking advantage of extraordinary luminosity at FCC-ee. The question how this measurement could influence searches of New Physics deserves separate studies.

For completeness, let us finally note that a very different and more straight forward way for identifying the neutrino species produced in Z decays would be to observe the interaction of the neutrinos within the FCC-ee detector. Indeed, with an integrated luminosity of 150 ab^{-1} at the Z -pole, some 2.4×10^{12} neutrinos are produced. Although this figure is large, unfortunately the charged current neutrino cross section with $E_\nu = 45 \text{ GeV}$ is low; $\sim 0.3 \text{ pb}$. Assuming a tracking area with 1 radiation length (which is far more than usual trackers) only ~ 3 interactions are expected. So this direct detection method seems unpractical, unless one develops a dedicated segmented detector with some $100 X_0$. We expect similar size effect in the spectrum of the ZRR photon.

4 Matrix element of KKMC

In the following numerical studies we shall use a version on **KKMC**, which features matrix element of the $e^+e^- \rightarrow \nu\bar{\nu} + n\gamma$ present in **KKMC** since version 4.19. The source code of the version 4.19 **KKMC** is available from <http://jadach.web.cern.ch/jadach/KKindex.html> or <http://192.245.169.66:8000/FCCeeMC/wiki/kkmc>.

The original 1999 version of **KKMC** of ref. [19] did not yet include a good quality matrix element for the neutrino pair production process. This is why during 1999/2000 LEP Physics Workshop [22], theoretical studies of the $\nu\bar{\nu}\gamma + n\gamma$ final states were based on **KORALZ** [23], **NUNUGPV** [24,25] and **GRC4F** [26,27] MC programs. The conclusion was at the time that predictions of these program can be trusted to within 2-3%. **KORALZ** has featured approximate matrix element for two real photons and approximate matrix elements for t channel W exchange (in case of ν_e), see also Ref. [28]. On the other hand **NUNUGPV** and **GRC4F**, have included exact matrix element for two photons, but soft photon resummation was implemented in **GRC4F** through a QED parton shower and in **NUNUGPV** through electron structure function formalism, instead of coherent exclusive exponentiation of ref. [19]. Both codes adopted methods to remove the double counting of radiation between matrix element and resummation. The virtual corrections to $\nu\bar{\nu}\gamma$ process were known from earlier work of Ref. [29] and used in some of these programs⁴.

Before the end of LEP era matrix element of **KKMC** for neutrino pair production process was upgraded and documented in a fine detail in Ref. [18]. In particular W -exchange diagram for electron neutrino channel was implemented and the electroweak (EW) library **DIZET**, the same as in **ZFITTER** [30], was added. The validity of the implementation of EW corrections in **KKMC** was cross-checked in this work by means of direct comparison of **ZFITTER** and **KKMC** for the $e^+e^- \rightarrow \nu\bar{\nu}$ process⁵ in spite that it is not seen experimentally.

Later on, in Ref. [31], the exact matrix element for $e^+e^- \rightarrow \nu\bar{\nu} + 2\gamma$ process (as

⁴Virtual corrections to W -exchange diagram were neglected in this work.

⁵ For the $e^+e^- \rightarrow \nu\bar{\nu}\gamma$ process EW corrections in **KKMC** enter in the soft photon approximation thanks to soft photon resummation.

implemented in KKMC) was also analysed in a great detail focusing on the delicate issue of the QED gauge invariance, especially in case of photon emissions out of the W boson exchanged in the t -channel.

The KKMC program is a general purpose MC event generator for producing pair of any kind of charged lepton (except electron), neutrino or quark. The $\mathcal{O}(\alpha^0)$ Born in KKMC is the $e^+e^- \rightarrow f\bar{f}$ process, completed with the $\mathcal{O}(\alpha^1)$, $\mathcal{O}(\alpha^2)$ QED corrections and $\mathcal{O}(\alpha^1)$ EW corrections. The case of neutrino is special because the $\mathcal{O}(\alpha^0)$ Born process $e^+e^- \rightarrow \nu\bar{\nu}$ is not visible in the detector, hence it is $e^+e^- \rightarrow f\bar{f}\gamma$ which can be treated as $\mathcal{O}(\alpha^0)$ Born process. (This kind of convention is used in NUNUGPV and GRC4F.)

In KORALZ and KKMC it is the $e^+e^- \rightarrow \nu\bar{\nu}$ process being the Born process, while $e^+e^- \rightarrow f\bar{f}\gamma$ is regarded as $\mathcal{O}(\alpha^1)$. Here and in the following we adopt the above convention. Matrix element of KKMC features the complete $\mathcal{O}(\alpha^2)$ QED corrections (instead of the $\mathcal{O}(\alpha^1)$ in case of Born being $e^+e^- \rightarrow f\bar{f}\gamma$). It means that KKMC includes exact matrix element for $e^+e^- \rightarrow f\bar{f}+2\gamma$ [31] and complete virtual corrections to $e^+e^- \rightarrow f\bar{f}\gamma$. Strictly speaking, as explained in Ref. [18], one-loop corrections to W -exchange contribution for the electron neutrino pair process in KKMC are taken in certain low energy approximation and will have to be improved in the future.

At the practical level, there is no possibility in KKMC to request through input parameters that at least one ZRR photon visible above certain minimum energy and angle (with respect to beams) is always present⁶ in the generated MC sample. One has to generate photons all over the entire phase space and then select a subsample of the events with one or more ZRR photons. This costs factor ~ 10 loss in terms of the CPU time for typical event selection of the ZRR process.

5 Monte Carlo results

Monte Carlo results in this Section were obtained in two KKMC runs at 105GeV and 161GeV with statistics of $\sim 4 \cdot 10^9$ weighted events. Figures 4 and 5, illustrate general features of the ZRR process.

Our event selection criteria for photons in the ZRR process include requirement of sum of the photon energies being above $0.10E_{beam}$, each photon angle with respect to incoming beam to be above 15° , and each photon transverse momentum being above $0.02E_{beam}$.

In the LHS plot of Figures 4 we see photon number distribution for all photons generated by KKMC for the $e^+e^- \rightarrow \nu\bar{\nu} + n\gamma$ process above IR cut-off $10^{-5}E_{beam}$ and for photons which pass the above criteria of the ZRR process. As we see, only $\sim 1\%$ fraction of ZRR events has two photons.

The RHS plot of Figure 4 presents the same two classes of MC events in the log of photon angle with respect to beams. The natural cut-off at $\theta \sim m_e/\sqrt{s}$ due to small but finite electron mass is clearly seen, and the ZRR cut-off at 15° is seen as well. The rejection rate from all MC events down to ZRR class is of order ~ 10 .

⁶This is due use of the basic MC algorithm for generating multiphoton events, the same as for other final fermions.

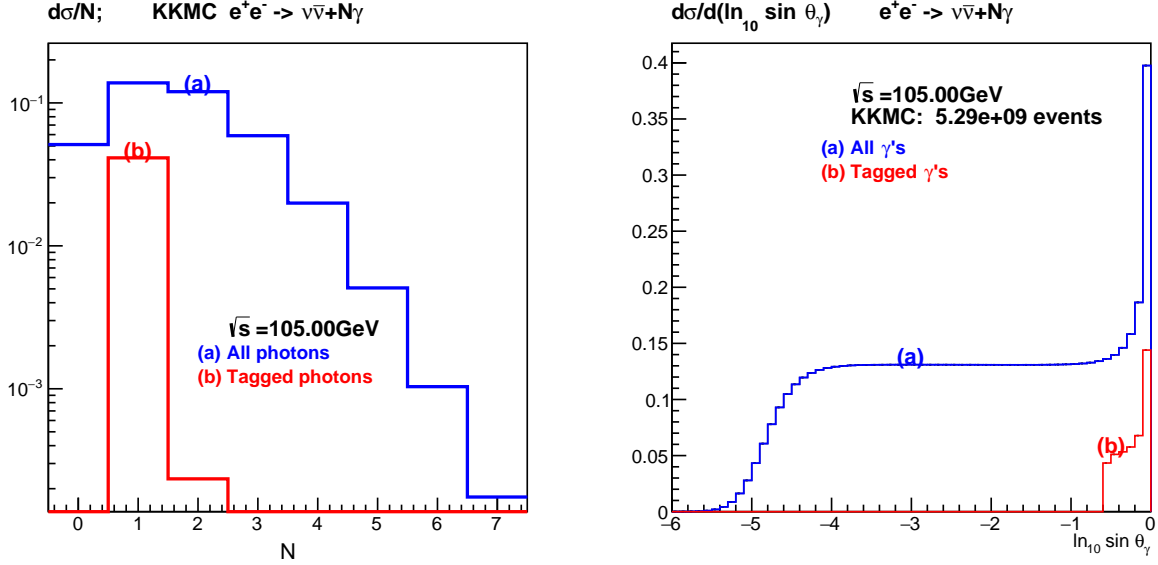


Figure 4: The distributions of photon multiplicity and photon angle in the process $e^+e^- \rightarrow \nu\bar{\nu}(N\gamma)$, $\nu = \nu_e, \nu_\mu, \nu_\tau$, (a) without restricting photons and (b) for ZRR subsample.

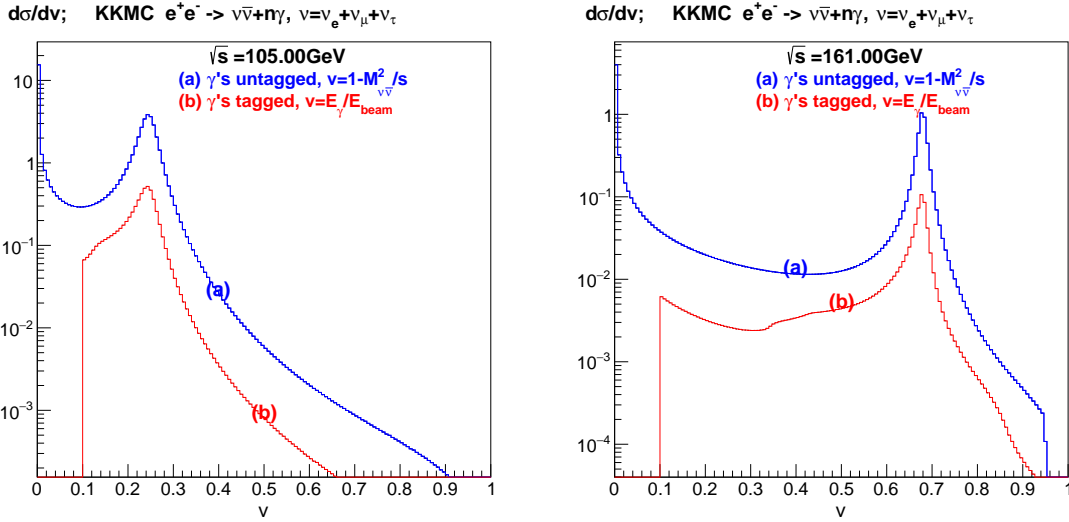


Figure 5: The distributions of photon energy in the processes $e^+e^- \rightarrow \nu\bar{\nu}(+n\gamma)$, $\nu = \nu_e + \nu_\mu + \nu_\tau$ (a) without restricting photons and (b) for ZRR subsample.

For completeness in Figure 5 we also show the entire distribution of the energy of all ISR photons and for visible photons in the ZRR MC sample for two energies, 105GeV and 161GeV.

Next, in Figure 6, we examine ZRR photon energy spectrum near the Z resonance, focusing on the W_t diagrams contribution, present in the electron neutrino case and

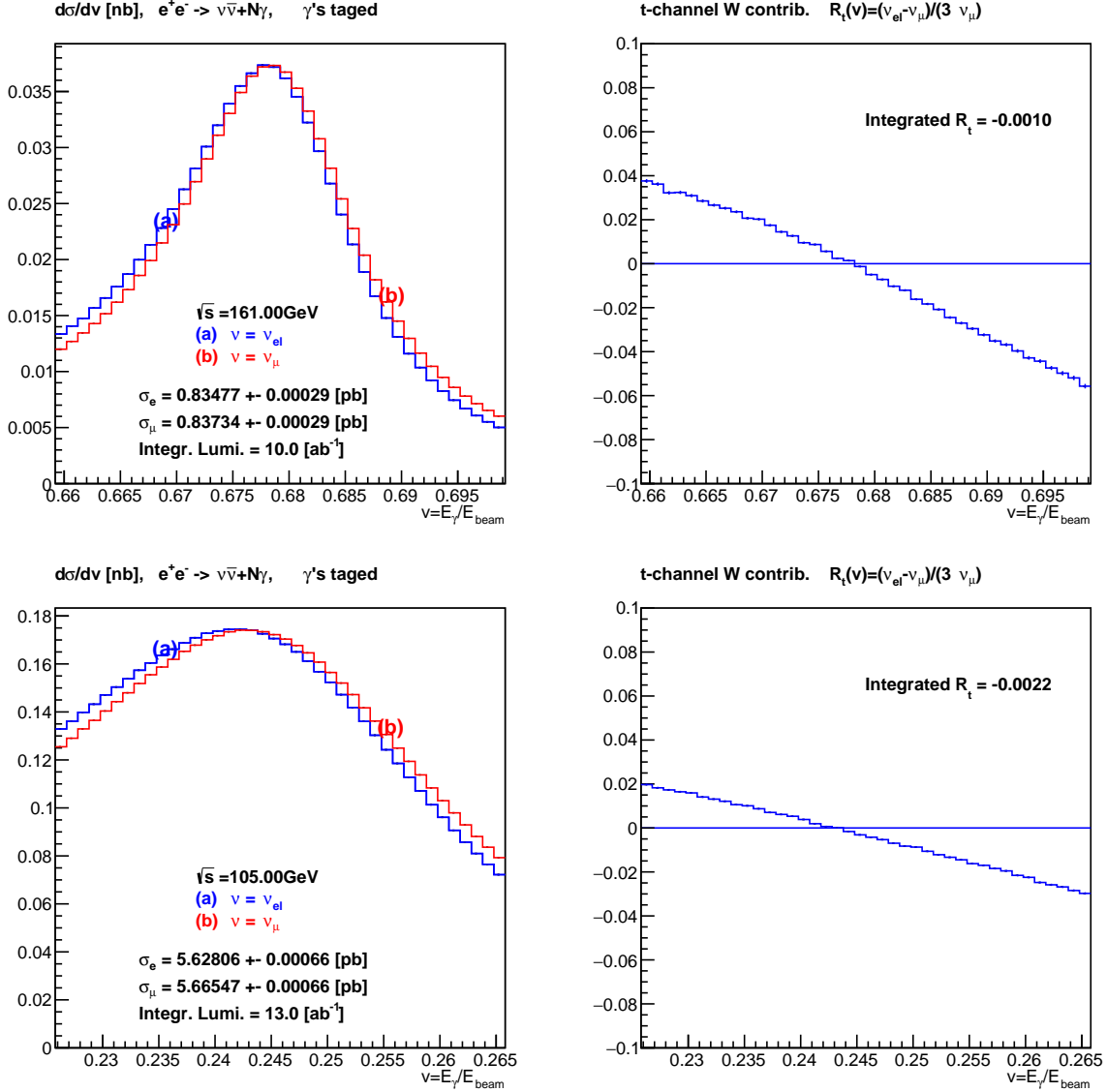


Figure 6: Examining difference of the ZRR photon spectrum for electron neutrino and muon neutrino channels due to t -channel W exchange.

absent for two other SM neutrinos. As compared to Born curve of Figure 3 the difference between electron and muon neutrino due to $Z_s \otimes W_t$ interference is roughly of the same size but slightly diluted. As expected, the Z resonance shape is deformed due to ISR/QED, increasing significantly the skewness of the resonance lineshape, in fact more than $W_t \otimes Z_s$ interference effect. Of course, ISR/QED effect can be subtracted using reliable Monte Carlo calculation for the ZRR process like KKMC.

Finally, in Figure 7 we examine how precisely one can deduce Z coupling to electron neutrino from the skewness of the ZRR spectrum near Z resonance for the anticipated

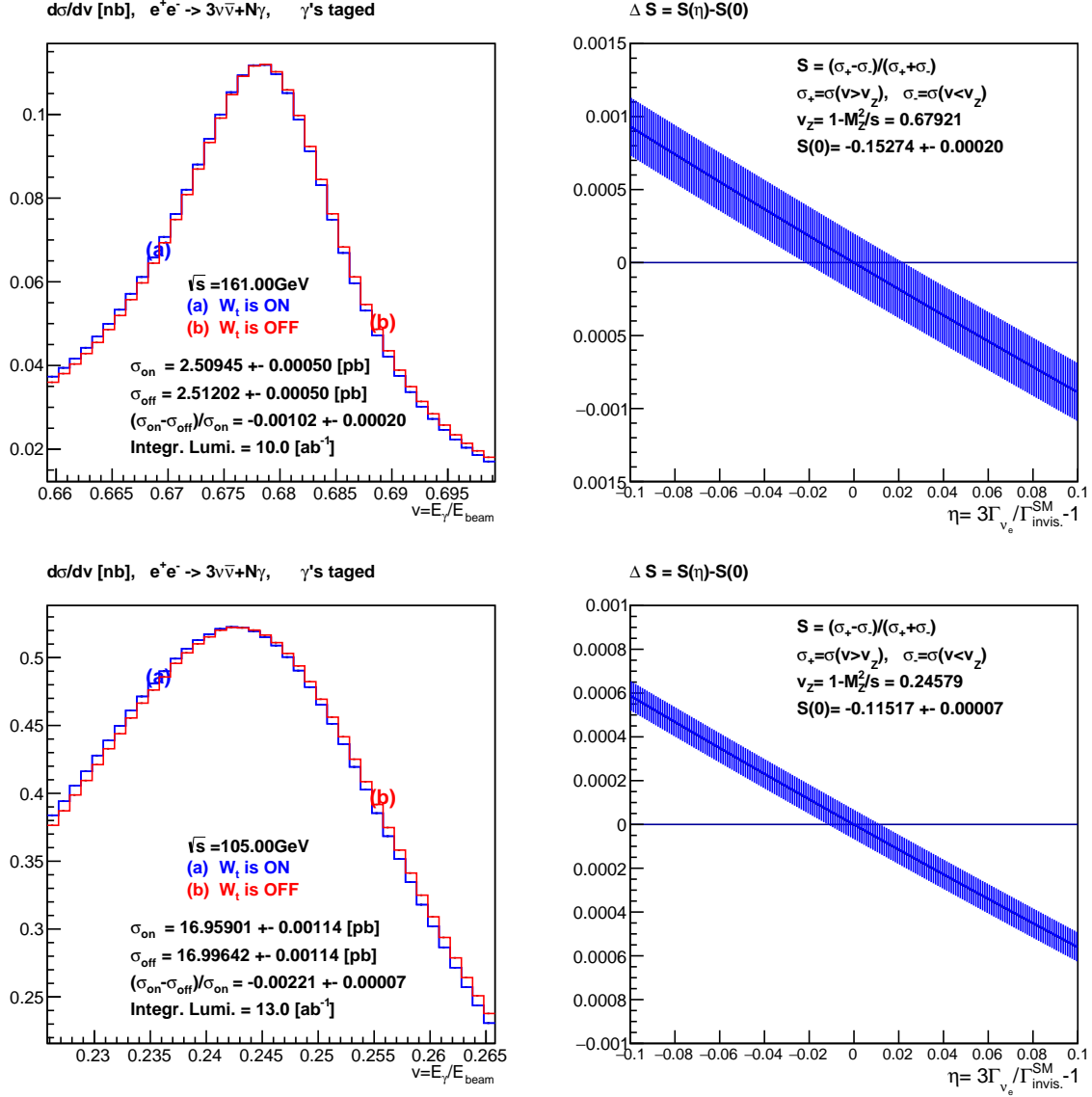


Figure 7: Examining difference of the ZRR photon spectrum for electron neutrino and muon neutrino channels due to t -channel W exchange.

FCC-ee integrated luminosity of 10ab^{-1} at 161GeV and 13ab^{-1} at 105GeV respectively⁷. The LHS plots of Figure 7 shows ZRR photon spectrum for all three neutrinos switching off and on $Z_s \otimes W_t$ interference, at two energies, 105GeV and 161GeV .

At $s^{1/2} = 161\text{GeV}$ the ZRR cross section integrated over the range $v_Z \pm 0.02$ of the plot is about 2.51pb . With the 10ab^{-1} integrated luminosity anticipated at FCC-ee, can be measure with the $\pm 5 \cdot 10^{-4}\text{pb}$ statistical error ($\pm 2 \cdot 10^{-4}$ relative error). The entire

⁷These integrated luminosities correspond to 2 years operation with 2 detectors at 161GeV and 6 months operation at 105GeV of FCC-ee.

$Z_s \otimes W_t$ interference effect in the integrated ZRR cross section is $22 \cdot 10^{-4}$ (relative) and is measurable. However, in order to determine $g_Z^{\nu_e}$ from it with the $\sim 1\%$ precision we have to exploit the parameter

$$S = \frac{\sigma(v > v_Z) - \sigma(v < v_Z)}{\sigma(v > v_Z) + \sigma(v < v_Z)} \quad (5.1)$$

parametrising the skewness of the Z resonance curve. In case of three neutrinos with equal SM couplings to Z , the prediction for the skewness parameter including QED effects and $Z_s \otimes W_t$ interference is $S = -0.15274 \pm 0.00020$, with its statistical error adjusted for 10ab^{-1} integrated luminosity⁸. In order to see how sensitive is the skewness S to $g_Z^{\nu_e}$ let us rescale Z couplings to neutrinos as in Eq. (3.3).

The corresponding change of $S(\eta)$ from the SM value $S(0)$ is presented⁹ in the RHS plots of Figure 7, together with the statistical error band for 10ab^{-1} integrated luminosity. From this figure it is easy to read the (statistical) precision of $g_Z^{\nu_e}$ at FCC-ee integrated luminosity is $\simeq 1\%$ at $s^{1/2} = 161\text{GeV}$ and $\simeq 0.5\%$ at $s^{1/2} = 105\text{GeV}$. This is the main and very interesting result of the present study.

The reference value of $S(0)$ is coming entirely from the precision SM calculation, hence it is important to know how much it is affected by the perturbative SM higher order corrections. In the above KKMC calculation the virtual $\mathcal{O}(\alpha^1)$ EW corrections for s -channel Z_s and γ_s exchanges from DIZET library were always switched on. In the additional MC run we have checked that switching off completely all $\mathcal{O}(\alpha^1)$ virtual EW+QCD corrections in KKMC (also vacuum polarization) causes shift of $S(0)$ by 0.0007. This is above the level of the experimental FCCee precision. However, due to smallness of EW and QCD couplings, we expect the size of unaccounted $\mathcal{O}(\alpha^2)$ non-QED corrections to $S(0)$ to be below 10^{-4} level. We keep in mind that for $Z_s \otimes W_t$ interference (dominant in $S(\eta)$), the present version of KKMC features virtual EW+QCD corrections of DIZET only for Z_s but not yet for W_t . Even for Z_s exchange, in the presence of hard photon, the EW virtual corrections of KKMC are still incomplete¹⁰.

In order to get an idea about the size of unaccounted higher order QED non-soft corrections in the SM prediction for $S(0)$ we have downgraded QED matrix element in KKMC by one order, to exponentiated $\mathcal{O}(\alpha^1)$ level, i.e. to $\mathcal{O}(\alpha^0)$ level for the ZRR process. This has induced shift in $S(0)$ only by $4 \cdot 10^{-4}$. The unaccounted non-soft QED $\mathcal{O}(\alpha^1)$ corrections to the ZRR process are suppressed by factor $2\frac{\alpha}{\pi} \ln \frac{s}{m_e^2} \simeq 0.12$, hence we expect them to be safely below the FCC-ee experimental precision $\sim 10^{-4}$.

6 Detector resolution effect

Let us now examine the effect of the detector resolution. To this end, we assume homogeneous calorimeter with a reasonably good energy resolution of :

⁸Statistical error in our MC runs was at least factor two smaller.

⁹ In fact we rescale the differences between ν_e and ν_μ ZRR distributions in Figures. 6 by $(1 + \eta)^{1/2}$. Near the Z peak $W_t \otimes Z_s$ interference dominates this difference and W contribution squared is negligible.

¹⁰Strictly speaking they are extrapolated out from the soft photon regime.

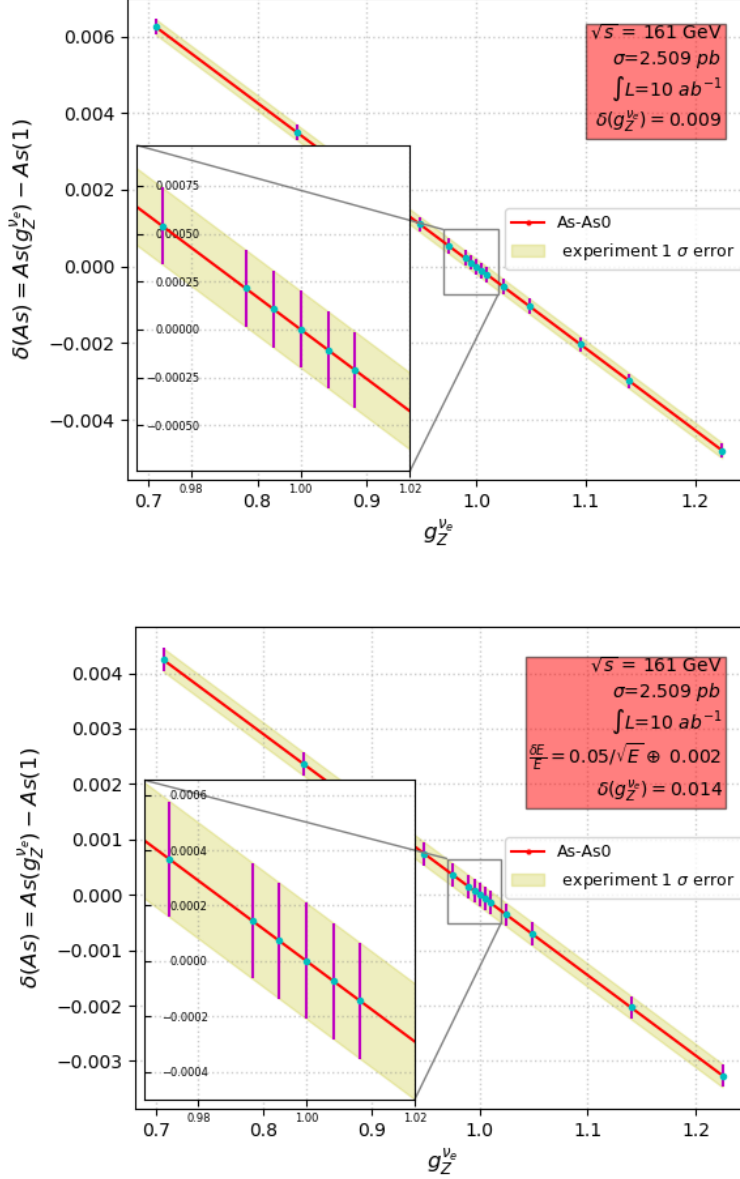


Figure 8: Experimental sensitivity of $g_Z^{\nu_e}$. Detector resolution effect off (left plot) and on (right plot). A 50% degradation is observed but the sensitivity still remains very good.

$$\frac{\sigma(E_\gamma)}{E_\gamma} = \frac{0.05}{\sqrt{E_\gamma}} \oplus 0.002 \quad (6.1)$$

The energy resolution of photons can be extracted experimentally from the reconstructed $\mu\mu\gamma$ events, for which the muons reconstructed angles are very precise. Thus one can achieve a 1C fit of such events and obtain a precise E_γ measurement, which is then compared to the energy measured with the calorimeter. This allows one to verify that the

energy scale is correct. With the resolution in equation (6.1), one observes as expected a degradation of the sensitivity on $g_Z^{\nu_e}$. However the sensitivity remains excellent at the level of 1.4 % as can be seen in Figure 8. With this error for $g_Z^{\nu_e}$ and assuming that N_ν will be measured with negligible error at FCC-ee and that there is no invisible new particles coupled to Z , one gets a sensitivity of 4.8% on $g_Z^{\nu_\tau}$ from equation 3.2 (the error on $g_Z^{\nu_\mu}$ from PDG was used).

Should the stochastic term be twice as worse (i.e. $0.1/\sqrt{E}$, which is typical for a sampling calorimeter), the sensitivity on $g_Z^{\nu_e}$ would be 2.4%. This "rapid" degradation implies that an excellent knowledge on the calibration of E_γ is crucial. Obviously a very good calorimeter energy resolution is very important for this measurement.

7 Summary and outlook

Main result of our study is that by means of exploiting interference between s -channel Z exchange and t -channel W exchange in the $e^+e^- \rightarrow X + \gamma$ process, the coupling constant of Z boson to electron neutrino and Z can be measured at the FCC-ee high luminosity with the statistical error of $\sim 1\%$, that is a factor ~ 20 better than the present error. The above result is obtained assuming observation of at least one photon with an angular distance from both beams above 15° and the energy above 10% of the beam energy. This important and encouraging result was obtained assuming integrated luminosity 10 and 13ab^{-1} for centre of the mass energy 161 and 105GeV. Keeping systematic error due to calorimeter energy resolution at the similar 1% level is within the reach of the available detector technology. It should be stressed that the above high precision requires comparison of experimental data with high quality Monte Carlo even generator, because multiphoton QED effects have to be removed in order to pin down the valuable $Z_s \otimes W_t$ interference effect.

The presented study is still preliminary and there is a number of issues requiring further studies: (1) virtual corrections for W_t contribution in KKMC matrix element has to be completed, (2) the size and shape of the QED deformation of the Z peak in ZRR obtained from KKMC should be cross-checked using independent calculation (3) calculating complete $\mathcal{O}(\alpha^2)$ EW loop corrections to $e^+e^- \rightarrow \nu\bar{\nu}$ process ($\mathcal{O}(\alpha^1)$ to ZRR $e^+e^- \rightarrow \nu\bar{\nu}\gamma$ subprocess) should be seriously considered, (4) dominant $\mathcal{O}(\alpha^3)$ QED non-soft corrections (in our convention) should be estimated/calculated.

There are also several other improvements in the analysis front, which needs to be studied, such as carrying a full fit of the ν spectrum instead of measuring its asymmetry and/or optimizing the ν range. Also, as already mentioned, study of the interference effect at low and high ν range¹¹ might be useful to improve the sensitivity on $g_Z^{\nu_e}$.

Acknowledgments

We would like to thank M. Skrzypek and Z. Wąs for useful discussions.

¹¹This would require introducing rescaling η parameter directly in the KKMC matrix element.

References

- [1] J. Lees, et al., [BaBar Collaboration], Phys. Rev. D88 (2013). [arXiv:1303.0571](#), [doi:10.1103/PhysRevD.88.072012](#).
- [2] J. Lees, et al., [BaBar Collaboration], Phys. Rev. D94 (2016). [arXiv:1609.06802](#), [doi:10.1103/PhysRevD.94.091101](#).
- [3] M. Huschle, et al., [Belle Collaboration], Phys. Rev. D92 (2015). [doi:10.1103/PhysRevD.92.072014](#).
- [4] R. Aaij, et al., [LHCb Collaboration], Phys. Rev. Lett. 115 (2015). [doi:10.1103/PhysRevLett.115.111803](#).
- [5] R. Aaij, et al., [LHCb Collaboration], Phys. Rev. D97 (2018). [arXiv:1711.02505](#), [doi:10.1103/PhysRevD.97.072013](#).
- [6] J.-T. Wei, et al., [Belle Collaboration], Phys. Rev. Lett. 103 (2009). [arXiv:0904.0770](#), [doi:10.1103/PhysRevLett.103.171801](#).
- [7] J. Lees, et al., [BaBar Collaboration], Phys. Rev. D86 (2012). [arXiv:1204.3933](#), [doi:10.1103/PhysRevD.86.032012](#).
- [8] R. Aaij, et al., [LHCb Collaboration], Phys. Rev. Lett. 113 (2014). [arXiv:1406.6482](#), [doi:10.1103/PhysRevLett.113.151601](#).
- [9] M. Tanabashi, et al., [Particle Data Group], Phys. Rev. D98 030001 (2018).
- [10] G. Voutsinas, E. Perez, M. Dam, P. Janot, Beam-beam effects on the luminosity measurement at LEP and the number of light neutrino species, Physics Letters B 800 (2020) 135068 (2020). [arXiv:1908.01704](#), [doi:https://doi.org/10.1016/j.physletb.2019.135068](#).
URL <http://www.sciencedirect.com/science/article/pii/S0370269319307907>
- [11] M. Bicer, et al., First Look at the Physics Case of TLEP, JHEP 01 (2014) 164 (2014). [arXiv:1308.6176](#), [doi:10.1007/JHEP01\(2014\)164](#).
- [12] M. Mangano, et al., Future Circular Collider, Vol. 1: Physics opportunities Submitted for publication to Eur.Phys.J.C. <http://cds.cern.ch/record/2651294> (2018).
- [13] M. Benedikt, et al., Future Circular Collider, Vol. 2: The Lepton Collider (FCC-ee) Submitted for publication to Eur.Phys.J.C. <http://cds.cern.ch/record/2651299> (2019).
- [14] B. Aharmim, et al., [SNO Collaboration], Phys. Rev. C72 (2005). [arXiv:0502021](#), [doi:10.1103/PhysRevC.72.055502](#).

- [15] S. Schael, et al., Precision electroweak measurements on the Z resonance, Phys. Rept. 427 (2006) 257–454 (2006). [arXiv:hep-ex/0509008](#), [doi:10.1016/j.physrep.2005.12.006](#).
- [16] G. Abbiendi, et al., Photonic events with missing energy in e^+e^- collisions at $S^{**}(1/2) = 189\text{-GeV}$, Eur. Phys. J. C18 (2000) 253–272 (2000). [arXiv:hep-ex/0005002](#), [doi:10.1007/s100520000522](#).
- [17] S. Jadach, M. Skrzypek, QED challenges at FCC-ee precision measurements (2019). [arXiv:1903.09895](#).
- [18] D. Bardin, S. Jadach, T. Riemann, Z. Was, Predictions for anti- ν ν gamma production at LEP, Eur. Phys. J. C24 (2002) 373–383 (2002). [arXiv:hep-ph/0110371](#), [doi:10.1007/s100520200948](#).
- [19] S. Jadach, B. F. L. Ward, Z. Was, The Precision Monte Carlo event generator KK for two fermion final states in e^+e^- collisions, Comput. Phys. Commun. 130 (2000) 260–325 (2000). [arXiv:hep-ph/9912214](#), [doi:10.1016/S0010-4655\(00\)00048-5](#).
- [20] M. Carena, A. de Gouvea, A. Freitas, M. Schmitt, Invisible Z boson decays at e^+e^- colliders, Phys. Rev. D68 (2003) 113007 (2003). [arXiv:hep-ph/0308053](#), [doi:10.1103/PhysRevD.68.113007](#).
- [21] J. Ellis, S.-F. Ge, H.-J. He, R.-Q. Xiao, Probing the Scale of New Physics in the $ZZ\gamma$ Coupling at e^+e^- Colliders (2019). [arXiv:1902.06631](#).
- [22] M. Kobel, et al., Two-Fermion Production in Electron-Positron Collisions, in: Proceedings, Monte Carlo Workshop: Report of the working groups on precision calculation for LEP-2 physics: CERN, Geneva, Switzerland, March 12-13, June 25-26, October 12-13 Oct 1999, 2000 (2000). [arXiv:hep-ph/0007180](#), [doi:10.5170/CERN-2000-009.269](#).
URL <http://weblib.cern.ch/abstract?CERN-2000-09-D>
- [23] S. Jadach, B. F. L. Ward, Z. Was, The Monte Carlo program KORALZ, version 4.0, for the lepton or quark pair production at LEP / SLC energies, Comput. Phys. Commun. 79 (1994) 503–522 (1994). [doi:10.1016/0010-4655\(94\)90190-2](#).
- [24] G. Montagna, O. Nicrosini, F. Piccinini, NUNUGPV: A Monte Carlo event generator for $e^+e^- \rightarrow \nu \text{ anti-}\nu \text{ gamma (gamma)}$ events at LEP, Comput. Phys. Commun. 98 (1996) 206–214 (1996). [doi:10.1016/0010-4655\(96\)00081-1](#).
- [25] G. Montagna, M. Moretti, O. Nicrosini, F. Piccinini, Single photon and multiphoton final states with missing energy at e^+e^- colliders, Nucl. Phys. B541 (1999) 31–49 (1999). [arXiv:hep-ph/9807465](#), [doi:10.1016/S0550-3213\(98\)00795-0](#).

- [26] J. Fujimoto, T. Ishikawa, T. Kaneko, K. Kato, S. Kawabata, Y. Kurihara, T. Munehisa, D. Perret-Gallix, Y. Shimizu, H. Tanaka, Grc4f v1.1: A Four fermion event generator for e^+e^- collisions, *Comput. Phys. Commun.* 100 (1997) 128–156 (1997). [arXiv:hep-ph/9605312](#), [doi:10.1016/S0010-4655\(96\)00126-9](#).
- [27] Y. Kurihara, J. Fujimoto, T. Ishikawa, Y. Shimizu, T. Munehisa, (grc neutrino neutrino gamma) Event generator for the single photon and double photon emission associated with neutrino pair production, *Comput. Phys. Commun.* 136 (2001) 250–268 (2001). [arXiv:hep-ph/9908422](#), [doi:10.1016/S0010-4655\(00\)00254-X](#).
- [28] P. Colas, R. Miquel, Z. Was, The Neutrino Anti-neutrino γ Cross-section and Invisible Width Measurement at LEP, *Phys. Lett. B* 246 (1990) 541–545 (1990). [doi:10.1016/0370-2693\(90\)90646-N](#).
- [29] M. Igarashi, N. Nakazawa, QED radiative corrections to the neutrino counting reaction e^+e^- , *Nucl. Phys. B* 288 (1987) 301–331, [Erratum: *Nucl. Phys. B* 294, 1180 (1987)] (1987). [doi:10.1016/0550-3213\(87\)90217-3](#).
- [30] D. Yu. Bardin, P. Christova, M. Jack, L. Kalinovskaya, A. Olchevski, S. Riemann, T. Riemann, ZFITTER v.6.21: A Semianalytical program for fermion pair production in e^+e^- annihilation, *Comput. Phys. Commun.* 133 (2001) 229–395 (2001). [arXiv:hep-ph/9908433](#), [doi:10.1016/S0010-4655\(00\)00152-1](#).
- [31] Z. Was, Gauge invariance, infrared / collinear singularities and tree level matrix element for $e^+e^- \rightarrow \nu(e) \text{ anti-}\nu(e) \gamma \gamma$, *Eur. Phys. J. C* 44 (2005) 489–503 (2005). [arXiv:hep-ph/0406045](#), [doi:10.1140/epjc/s2005-02381-y](#).